Open Access

Research Article

PRNANO

Precis. Nanomed. 2024, 7(4):1348-1364

ANDOVER HOUSE

Self-assembled Human Serum Protein-based Core-shell Nanoparticles to Inhibit Key Oncogenic Signaling in Drug-Resistant Leukemia

Archana Payickattu Retnakumary[1†], Lekshmi G Kumar[1†], Neeraj Sidharthan[2], Pavithran Keechilat[2], Giridharan L. Malarvizhi[1], Prasanna L. Hanumanthu[1], Madhavan V. Thampi[3], Deepthy Menon[1], Krishnakumar Menon[1], Shantikumar Nair[1] and Manzoor Koyakutty[1*]

[1]*Amrita Centre for Nanosciences and Molecular Medicine, Amrita Vishwa Vidyapeetham, Cochin, India*

[2]*Dept. of Medical Oncology,*

[3]*Dept. of Human Cytogenetics, Amrita Institute of Medical Science and Research Centre, Amrita Vishwa Vidyapeetham, Cochin, India*

Submitted: September 15, 2024 Accepted: October 26, 2024 Published: November 1, 2024

Graphical Abstract

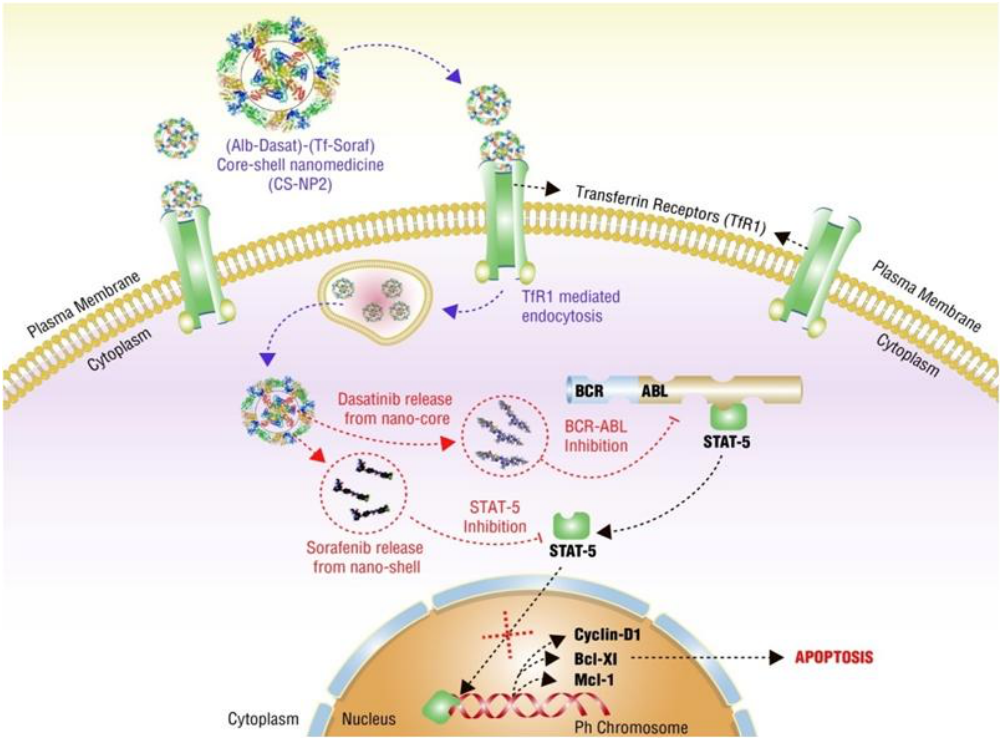

Abstract

Simultaneous inhibition of multiple oncogenic signaling pathways is crucial for managing refractory cancers. This study introduces two unique core-shell nanoparticle (CS-NP) systems crafted from natural proteins, simultaneously targeting two crucial oncogenic pathways in refractory chronic myeloid leukemia (CML). Molecular analysis of approximately 14 refractory CML patients identified resistance to the standard treatment drug, imatinib, attributed to the overexpression of the STAT5-transferrin pathway alongside the classic BCR-ABL fusion gene. To address this, we developed two dual-drug-loaded

*Corresponding authors: Manzoor Koyakutty: manzoork@aims.amrita.edu, Shantikumar Nair: shantinair@aims.amrita.edu

† *These authors contributed equally to the work*

core-shell nanoparticles: (a) CS-NP1: Protamine sulfate nanocores carrying BCR-ABL siRNA and an albumin shell loaded with the STAT5 inhibitor sorafenib, denoted as (PS-siRNA)-(Tf-Soraf) CS-NP; (b) CS-NP2: features a second-generation BCR-ABL inhibitor, dasatinib, in the albumin nanocore, and sorafenib in the transferrin nanoshell, labeled as (nAlb-Dasa)-(Tf-Soraf). We hypothesized that these dual-drug-loaded CS-NPs would effectively target both BCR-ABL and STAT5 pathways, with the transferrin nanoshell aiding in precise delivery to refractory CML cells overexpressing TfR1 due to STAT5 activity. Initial evaluations in drug-resistant CML cell lines and patient-derived cells demonstrated significant cytotoxicity. Remarkably, even patients with BCR-ABL oncogene mutations displayed over 95% cytotoxicity with the CS-NPs. Furthermore, *in vivo* testing on a human xenograft model with a BCR-ABL+/+/STAT5+/+/TfR+/+ phenotype showcased a strong anti-tumor response. These results underscore the potential of a molecular-diagnosis-based rational design approach for protein-protein core-shell nanoparticles to simultaneously inhibit multiple oncogenic pathways, thereby overcoming resistance to targeted molecular therapies.

Keywords: Core-shell nanoparticles, albumin, transferrin, si-RNA, Tyrosine kinase inhibitors, Imatinib, Sorafenib, drug resistance, chronic myeloid leukemia

Purpose, Rationale, and Limitations

This study is motivated by the potential of core-shell nanomedicines to address the challenge of highly resistant cancers where more than one molecular driver mechanism is critically aberrant. Imatinib-resistant/refractory chronic myeloid leukemia (CML) is one of the most appropriate cancer models to demonstrate how to address multiple oncogenic pathways using nanoparticles. The molecular characterization of CML patients showed a consistent overexpression of STAT5 and its transcriptional target-transferrin receptors (TfR1) in the leukemic cells isolated from the blood/bone marrow samples. These molecular aberrations were irrespective of the mutation/overexpression of the BCR-ABL kinase, exemplifying the need to target these proteins, thereby simultaneously eliciting a favorable therapeutic response. The purpose of the current study was to establish the *in vitro* and *in vivo* proof-of-concept of the dual targeting of BCR-ABL and STAT5 using core-shell nanoparticles prepared from endogenous proteins with BCR-ABL-targeting drug/siRNA loaded in the nanocore and STAT5-targeting sorafenib loaded in the nanoshell. This study is limited by patient sample availability and the detailed molecular characterization of the cells following the core-shell nanoparticle treatment. Furthermore, using a subcutaneous model to study the efficacy of nanomedicine in a hematological malignancy is a potential limitation of the study.

Introduction

Molecularly targeted tyrosine kinase inhibitors (TKIs) are a crucial class of cancer therapeutics due to their specificity for cancer-driver mechanisms, which generally results in better safety profiles than DNA-intercalating agents.[1,2] However, drug resistance to TKIs, often caused by point mutations in the target gene, remains a significant challenge. For example, the T790M gatekeeper mutation prevents the target-binding of epidermal growth factor receptor (EGFR) inhibitors such as gefitinib and erlotinib[3]; the T315I mutation in the BCR-ABL kinase confers resistance to imatinib,[4] and the L1196M gatekeeper mutation in anaplastic lymphoma kinase (ALK) induces resistance to Crizotinib.[5] Simultaneous targeting of multiple pathways can significantly reduce the likelihood of developing resistance in various cancers. This approach diminishes the risk of disease relapse by addressing heterogeneous cell populations within a tumor at lower doses of each drug, thereby reducing toxicity and improving patient tolerance and adherence to therapy.[6,7] More importantly, it allows for the customization of treatment strategies based on the individual characteristics of each patient.

Innovatively designed nanosystems offer advanced solutions to complex issues in diseases such as cancer. Several research groups, including ours[8,9] have demonstrated the potential of nanosystems to deliver multiple drugs simultaneously to cancer cells. In addition to enabling cell-specific targeting, nano-encapsulation improves drug solubility and stability, enhances efficacy, and reduces side effects.[10] It also allows for controlled drug release, thus maintaining a sustained therapeutic effect. Precisely engineered nanoparticles can deliver multiple drugs, exploiting synergistic effects where the combined therapeutic impact exceeds the sum of the individual effects.[11–13] For instance, cell membrane-coated mesoporous silica core-shell nanosystems loaded with daunorubicin and a TGFβ-RII neutralizing antibody have been

shown to overcome chemo-resistance in leukemia treatment effectively.[10] Our group has also reported successfully using protein-polymer core-shell nanoparticles for delivering dual drugs in drug-resistant cancers.[14–16]

Here, we demonstrate two distinct core-shell nanoparticles designed for the simultaneous delivery of drugs targeting both BCR-ABL and STAT5 in refractory CML. Imatinib resistance in CML is primarily driven by mutations or amplification of the BCR-ABL oncogene.[4,17,18]Although imatinib (IM) effectively inhibits BCR-ABL in the chronic and early accelerated phases, a significant proportion of patients develop resistance due to kinase domain mutations and BCR-ABL gene amplification.[19–21] Efforts to address this limitation with second- or third-generation inhibitors such as dasatinib (DS), nilotinib (NL), bosutinib, or ponatinib have encountered challenges due to high toxicity and single-target specificity, which are inadequate in the presence of heterogeneous cell populations with alternative survival mechanisms.[22–29] These newer drugs primarily target BCR-ABL, leaving unaddressed other molecular mechanisms in refractory CML.[30]

Recent insights into alternative pathways reveal that, besides BCR-ABL, patients may experience oncogene-independent disease progression through the STAT family of transcription factors.[31–34] Although BCR-ABL can activate STAT5 under certain conditions, STAT5 can also contribute to BCR-ABL-independent disease progression and resistance, making it essential for the survival and maintenance of leukemic cells, particularly in refractory cases.[35–43] Based on these findings and the molecular characterization of patients from our hospital, the Department of Hematology and Oncology at Amrita Institute of Medical Sciences, Kochi, we developed the following nanosystems to inhibit two different driver mechanisms simultaneously: BCR-ABL and STAT5 in refractory CML:

a) A core-shell nanosystem with a protamine nanocore carrying BCR-ABL siRNA and an albumin nanoshell loaded with a potent STAT5 inhibitor sorafenib. The albumin nanoshell was conjugated to transferrin to enable targeted delivery of the payload to CML cells, which overexpressed the transferrin receptor (TfR1), especially at blast crisis.

b) Another core-shell nanosystem with clinically used second-generation BCR-ABL inhibitor dasatinib loaded in the albumin nanocore and sorafenib in the transferrin nanoshell. As siRNA was not a clinically approved therapeutic option, we believe dasatinib will provide a translational product.

In both cases, the core-shell nanosystem exhibits inherent specificity for cancer cells, as the transferrin shell preferentially binds to TfR1 overexpressed in refractory CML. The rationale for using the transferrin ligand stems from the molecular diagnosis of approximately 14 imatinib-resistant CML patients, who exhibited consistent upregulation of STAT5 and its transcriptional target TfR1. Both systems demonstrated excellent cellular internalization and cytotoxicity in cell lines. When tested in patient samples, the CS-NPs showed toxicity even in highly refractory patient-derived cells, including those with point mutations in the BCR-ABL oncogene (T315I, G250E, F311I). The anti-tumor response generated by these nanoparticles in a mouse xenograft model with a BCR-ABL$^{+/+}$/STAT5$^{+/+}$/TfR$^{+/+}$ phenotype supports the hypothesis of dual-drug targeting in aberrant cancer types. This work highlights the significance of a multi-targeted nanoparticle strategy tailored to the molecular profile of individual patients, advancing treatment efficacy, reducing side effects, and bringing us closer to personalized medicine.

Materials and Methods

Materials

K562 cells (NCCS, Pune), RPMI medium, Fetal Bovine Serum(Gibco, USA), Albumin, Protamine, and transferrin (Sigma Aldrich USA), Chloroauric acid ($HAuCl_4$) (Spectrochem, India), HCl (Qualigens, India), Stemspan culture medium (Stem Cell Technologies, USA), Matrigel (Corning, Sigma Aldrich, USA), Annexin V/PI apoptosis detection kit (BD Biosciences, USA), Primers (Sigma Aldrich, USA), Antibodies (BD Biosciences, USA), Bacterial lipopolysaccharide (Sigma Aldrich USA) were used for the study.

Methods

Cell culture and development of IM-resistant K562R cells: K562R cells were developed as described in the supplementary section. The

cells were cultured in RPMI-1640 (Sigma Aldrich, USA) with 10% fetal bovine serum (FBS) (Gibco, USA), 1% L-glutamine (Sigma Aldrich, USA), and 1% penicillin/streptomycin (Gibco, USA). Cells were maintained at 37 0C with 5% CO2 used for further studies.

Isolation and characterization of patient-derived leukemic mononuclear cells: Blood/bone marrow samples were collected from 14 CML patients who reported at the Department of Hematology and Oncology at Amrita Institute of Medical Sciences Health Science Campus from 2011 to 2013. The samples were collected in BD Vacutainer® EDTA Tubes (BD, USA) after obtaining informed consent from the patients and approval from the Institutional Human Ethics Committee of Amrita Institute of Medical Sciences and Research Centre, Kochi, India. All methods were performed following institutional guidelines and regulations. The mononuclear cells were isolated using density gradient centrifugation. FISH analysis for BCR-ABL, gene expression for BCR-ABL and STAT5, and IM resistance mutation analysis (IRMA) were performed.27 (Details given in Supplementary section).

Design, development, and characterization of CS-NPs: CS-NPs were designed in-silico using AutoDock and wet-chemically synthesized using sequential protein nano-precipitation chemistry as reported by our group earlier but with minor modifications (preparation details given in Supplementary section).38-40 Characterization of the nanoparticles was performed using dynamic light scattering (DLS) (DLS, Nano ZS, Zetasizer—Nano series, Malvern, UK), SEM (SEM-JSM-6490LA (JEOL, Japan)), confocal microscopy (Leica TCS SP5 II, Germany), and high-performance liquid chromatography (Shimadzu, Japan). The cytotoxicity of CS-NPs was assessed in cell lines and patient samples using MTT and apoptosis (Annexin V/PI) assay. Gene expression studies using qRT-PCR were conducted to determine the downregulation of BCR-ABL and Mcl-1 (Details given in the Supplementary section).

In vivo studies: The anti-tumor efficacy of both the CS-NPs was tested in a subcutaneous xenograft model developed in Swiss Albino nu/nu. (Details are provided in the Supplementary section.)

Statistical analysis: The reproducibility and validity of the results were ensured by performing sufficient biological replicates wherever possible. Data are expressed as means ± SD, and the images represent the experiments conducted. The paired 1-tailed Student's t-test was used to examine differences between the means of the two groups. Statistical analyses were performed using PRISM software. 'p' values of < 0.05 were considered statistically significant.

Results and Discussion

Refractory CML Exhibits High Levels of STAT5 and TfR1, Along with Amplified BCR-ABL

The refractory cell line K562R, developed in our lab by prolonged treatment of a low dose of IM, demonstrated imatinib insensitivity up to 75 µM (Supplementary Figure S1). Our previous studies indicated that imatinib resistance in K562R cells was not associated with the drug efflux protein P-gp or point mutations in the kinase domain (REF). Instead, resistance was linked to the overexpression of BCR-ABL and STAT5. De Groot et al. previously showed that BCR-ABL activates STAT5 independently of JAK2 and that STAT5 transcriptional regulation is critical for maintaining K562 leukemia cells.[44] However, STAT5 becomes a crucial regulator of cell survival in later resistance stages and functions independently of BCR-ABL.[45]

We observed that the expression of TfR1, a transcriptional target of STAT5, was approximately three times higher in the K562R cell line compared to the imatinib-sensitive K562S cell line. TfR1 is the receptor responsible for the endocytosis of transferrin-bound iron, essential for cell cycle progression, DNA replication, and the mitochondrial electron transport chain.[46] Several studies have highlighted that iron metabolism is significantly disrupted in cancer, contributing to disease progression and drug resistance.[47] Zhu et al. previously identified TfR1 as a STAT5 target gene, noting that STAT5-null mice exhibited microcytic hypochromic anemia associated with downregulation of TfR1.[48] Furthermore, Kerenyi et al. investigated the role of STAT5 in regulating iron uptake through iron regulatory proteins IRP-2 and TfR1, a finding confirmed by our studies.[49] We observed a significant reduction in TfR1

expression when cells were treated with the STAT5 inhibitor sorafenib (Supplementary Figure S2), providing evidence for the BCR-ABL-STAT5-TfR1 crosstalk.

Although TfR1 has been reported as a potential biomarker for disease aggressiveness and is widely used for cell-specific targeting of therapeutic payloads, its critical role in molecular drug resistance in CML has been less explored, except in a few studies related to adriamycin resistance in K562 cells.[50] We investigated this key interaction between BCR-ABL, STAT5, and TfR1 in patient samples. Supplementary Table 1 lists the selected patients, classified according to European Leukemia Net recommendations.

FISH analysis data in **Figure 1A** revealed the characteristic t(9;22) translocation in all 14 patients, with multiple copies observed in patient P12. qRT-PCR studies showed that, in addition to BCR-ABL, STAT5 transcript levels were also upregulated, particularly in refractory patients P5-P14, compared to the drug-sensitive cases P1-P4 (**Figure 1B**). IRMA identified clinically relevant BCR-ABL point mutations in three patients: P7 (F311I, phenylalanine → isoleucine), P8 (T315I, threonine → isoleucine), and P13 (G250E, glycine → glutamic acid), suggesting the involvement of alternative signaling mechanisms in kinase inhibitor resistance.

Interestingly, while TfR1 expression in chronic phase patients (P1-P4) ranged from 2–8%, it was significantly higher in the cells isolated from imatinib-resistant patients (P5-P14), ranging from 12.9 to 60.0% (**Figure 1C**). This increase in TfR1 expression correlated with elevated levels of BCR-ABL and STAT5. However, there was no clear correlation between TfR1 expression and specific BCR-ABL point mutations; for instance, P7 (F311I) had a TfR1 expression of 16.7%, P8 (T315I) had 22.4%, and P13 (G250E) had 60.1%. Thus, similar to the results observed in K562R cells, refractory patient samples also exhibited predominant upregulation of STAT5 along with BCR-ABL, independent of point mutations in the BCR-ABL domain. Compared to chronic phase patients (P1-P3), BCR-ABL and STAT5 expression levels were progressively higher in patients who had lost response or developed resistance to imatinib (P4-P7 and P8-P14).

Based on the molecular characterization of cells from refractory patients, we hypothesize that targeting STAT5 and TfR1 in conjunction with BCR-ABL may provide better therapeutic outcomes in refractory CML rather than focusing solely on BCR-ABL. Additionally, leveraging TfR1 overexpression in refractory cases could enable more specific drug delivery using transferrin as a nanoparticle-targeting ligand.

Preparation and Characterization of CS-NP1: (PS-siRNA)-(Tf-Sorafenib)

Considering the significant overexpression of STAT5 and BCR-ABL and the correlated involvement of TfR1 in refractory patient samples, we prepared nanotherapeutics targeting BCR-ABL and STAT5 using a single core-shell nanoparticle (CS-NP1). The core carries an anti-BCR-ABL siRNA, and the nanoshell contains an anti-STAT5 molecule, sorafenib. The transferrin-based nanoshell enhances the targeted uptake of the CS-NP in CML.

Previous studies have shown that therapeutic siRNAs targeting BCR-ABL effectively downregulate BCR-ABL expression and induce apoptosis in highly resistant patient cells.[52]

We observed that sorafenib underwent spontaneous irreversible binding with transferrin, embedding itself in the hydrophobic core of transferrin. *In-silico* modeling (**Figure 2A**) indicated that sorafenib interacts primarily with cysteine and arginine residues of transferrin through hydrophobic interactions, with a binding energy (BE) of −6.69 kcal/mol, enabling approximately three sorafenib molecules per transferrin (**Supplementary Figure S3A**). We also assessed whether sorafenib loading in transferrin affected the Tf-TfR1 binding affinity. *In-silico* results showed that the sorafenib binding site in transferrin differs from that of TfR1 (**Figure 2B**).

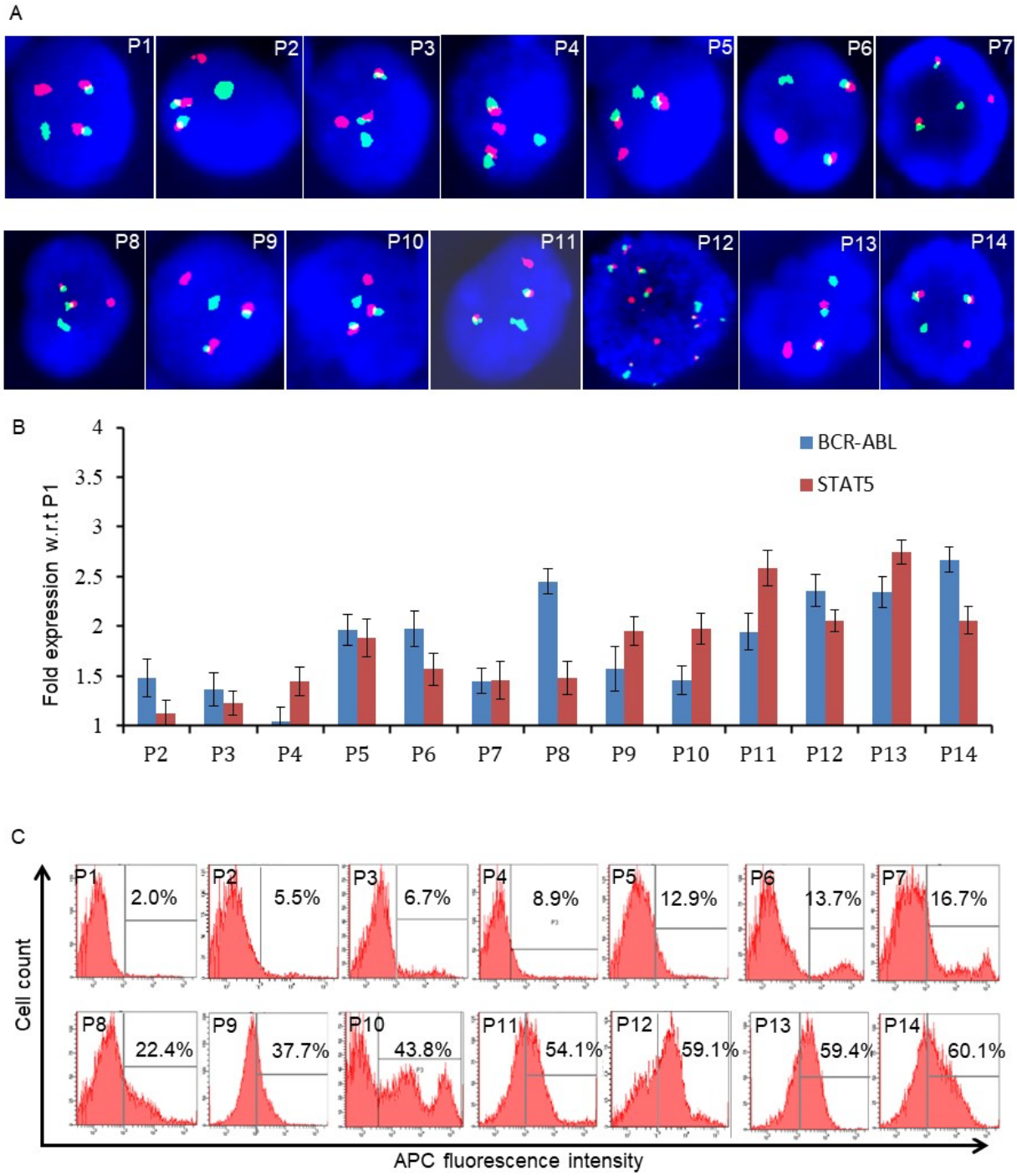

Figure 1. Molecular characterization of chronic myeloid leukemia (CML) patients shows overexpression of BCR-ABL and STAT5 in refractory cases with correlative overexpression of TfR1. (A) FISH analysis shows a typical pattern of BCR-ABL fusion in all 14 patients. (B) BCR-ABL and STAT5 expression profile of CML patients using RT-PCR. P1 was taken as the calibrator, and all other patient samples were plotted as fold expressions with respect to P1. The endogenous control was GAPDH. (C) A representative flow-cytogram showing TfR1 expression in CML patients shows an interesting correlative overexpression of TfR1 with drug resistance/STAT5 expression. TfR1 expression was measured using activated protein C conjugated monoclonal antibody against TfR1. This data is consistent with other reports highlighting the role of STAT5 in refractory CML.[51]

The TfR1-(Tf-Soraf) interaction recorded a BE −5.86 kcal/mol, comparable to Tf-TfR1; −5.81 kcal/mol. The CS-NP formulations were synthesized at 4°C to prevent the degradation of siRNA. Once prepared, the samples were stored at −20°C for up to one month. The nanoparticle size, stability, and cytotoxicity remained unchanged without any significant changes for up to one month *(data not included)*. Experimental studies confirmed that the intracellular uptake of Tf-Soraf was approximately twice that of free sorafenib, indicating more specific delivery through TfR1 (**Supplementary Figure S3B**). Notably, sorafenib's release from the nanoshell was minimal, even after 21 days (**Supplementary Figure S3C**), suggesting that the transferrin nanoshell effectively binds sorafenib and may prevent its premature release during circulation.

We used a cationic polypeptide, protamine sulfate, which forms complexes with nucleic acids through electrostatic interactions for the siRNA nanocore.[53] Protamine also facilitates cellular uptake due to its positive charge and promotes endolysosomal escape via the proton sponge effect, protecting the therapeutic payload from enzymatic degradation.[54] As anticipated, protamine spontaneously complexed with siRNA, forming a robust nanocore that was subsequently conjugated with the Tf-Soraf-nanoshell. **Figure 2C** shows the schematic representation of (PS-siRNA) -(Tf-Soraf) CS-NP, hereafter referred to as CS-NP1. Transmission electron microscopic (TEM) imaging confirmed the core-shell architecture similar to the *in-silico* model. DLS indicated a size range of 10–40 nm for the PS-siRNA nanocore (**Figure 2D**), while atomic force microscopy (AFM) revealed a spherical shape with a size of approximately 20 nm (**Figure 2E**). The encapsulation efficiency of siRNA in the nanocore was around 60%. DLS further showed a size increase to approximately 225 nm, confirming the formation of CS-NP structure (**Figure 2F**). TEM also displayed the Tf-nanoshell on the surface of the PS-siRNA nanocore (**Figure 2G**).

The serum stability study (**Figure 2H**) indicated that siRNA in the nanocore remained complexed with the protamine and was stable irrespective of its incubation with serum (50% FBS at 37°C) (lanes 3, 4). However, the sample remained in the well despite reducing the percentage of the agarose gel (2%). A similar observation was also reported previously.[55] We presume this happened because of the tight packaging of negatively charged siRNA by positively charged protamine, and the PS-siRNA nanocore had a positive charge, which prevented its mobility in the gel. In contrast to this observation, free siRNA degraded within 48 hours (lane 2). With this experiment, we ensured the tight packaging of siRNA in the protamine nanocore, which remained stable under physiological conditions.

To evaluate the efficacy of the core-shell nanosystem, we prepared two systems with varying siRNA concentrations: CS-NP1a with 2 nM siRNA in the PS-siRNA nanocore and CS-NP1b with 5 nM siRNA. In both formulations, the Tf-Soraf nanoshell contained 10 μM sorafenib. For cellular uptake studies, the Tf-nanoshell was doped with 25-atom clusters of fluorescent gold (Au) using our previously published protocol, enabling tracking via fluorescence imaging.[56] TfR1-targeted uptake of CS-NPs was observed in most cells (**Figure 2I**). The cells were washed twice before the images were captured to ensure the absence of uninternalized particles adsorbed on the surface of the cells. Flow cytometry confirmed this uptake, with approximately 60% of cells showing Au fluorescence (**Supplementary Figure S4**). The targeted uptake was further confirmed by pretreating cells with excess Tf or inhibiting endocytosis at 4°C, which drastically reduced uptake to less than 2%, indicating that CS-NP1 was specifically endocytosed in CML cells via TfR1. Importantly, less than 10% of healthy peripheral blood mononuclear cells showed uptake of CS-NP1, demonstrating that the preferential uptake in CML cells was due to TfR1 overexpression. However, we couldn't perform the internalization dynamics of Tf-Soraf in the cells. Comparing the data in **Supplementary Figure S3B** and the flow cytometry data in **Supplementary Figure S4**, we presume that the internalization can happen between 30 min and 2 h.

CS-NPs Exhibited Combinatorial Toxicity in Refractory CML Cells by Simultaneous Inhibition of BCR-ABL and STAT5

In vitro, the nanocore, nanoshell, and CS-NPs were characterized separately. Initially, we assessed the efficacy of the PS-siRNA nanocore in silencing the BCR-ABL oncogene and inducing cytotoxicity in K562R cells (**Figure 3A**). The siRNA nanocore demonstrated a dose-dependent cell death, and the IC50 was 2 nM after 48 h of treatment. Nearly 80% cell death was observed at a concentration of 5nM. Apoptosis assay further validated this, which showed approximately 46.3% of cells undergoing apoptosis upon treatment with 2 nM PS-siRNA (**Figure 3B**). PS-siRNA treatment also induced a concomitant reduction in mRNA expression in K562R cells. The mRNA expression levels were 18.51%, 10.4%, 5.8%, and 0.08% with 1, 2, 5, or 10 nM siRNA, respectively (**Figure 3C**).

Next, we evaluated the effect of the Tf-Soraf nanoshell alone. **Figure 3D** demonstrates that Tf-Soraf induced dose-dependent and enhanced toxicity in K562R cells at 10-20 µM compared to free sorafenib. The apoptosis assay revealed that approximately 56.1% of cells underwent apoptosis when treated with 10 µM of Tf-Soraf (**Figure 3E**). Since STAT5 is a transcriptional regulator of the anti-apoptotic protein Mcl-1, we studied the expression of Mcl-1, which showed a concomitant downregulation upon Tf-Soraf treatment.

To compare *in vitro* efficacy, we tested CS-NP1a (2 nM siRNA) and CS-NP1b (5 nM siRNA) on K562R cells, with sorafenib in the nanoshell kept constant at 10 µM for both formulations. Cell viability results (**Figure 3G**) indicated that CS-NP1a reduced cell viability to approximately 30.53%, compared to 60.12% with the nanocore alone and 50.34% with the nanoshell alone. Flow cytometry data (**Figure 3H**) showed about 79.8% cell death with CS-NP1a and approximately 84.1% cell death with CS-NP1b. These results suggest that the simultaneous inhibition of BCR-ABL and STAT5 using CS-NP1 resulted in enhanced toxicity in imatinib-resistant K562R cells, compared to that induced by either PS-siRNA or Tf-Soraf shell alone.

CS-NPs Induce Enhanced Cytotoxicity in Leukemic Bone Marrow Progenitors While Sparing Healthy Blood Cells

We assessed the hemolytic potential of CS-NPs using whole blood from healthy donors. Both CS-NPs were found to be non-hemolytic (**Supplementary Figure S5A**). Additionally, the proinflammatory cytokine response to CS-NPs was evaluated in healthy human peripheral blood mononuclear cells (PBMCs), showing no significant effects compared to the untreated control (**Supplementary Figure S5B**). The nanoparticles did not affect the viability of healthy mononuclear cells (**Supplementary Figure S5C**) at the concentrations used in CML patient samples, indicating the hemocompatibility of the CS-NP system and the retention of molecular specificity of the small molecules.

Next, we tested CS-NPs in patient-derived CML cells (n=14). **Figure 4** illustrates the cytotoxicity of NP-treated primary leukemic cells from CML patients with varying imatinib (IM) resistance levels. Clinical data (**Supplementary Table 1**) showed that patients P1-P3, in the chronic phase, responded well to an IM dose of 400 mg/day. Patients P4-P7 initially responded to IM but later exhibited a loss of response. Patients P8-P14 were refractory, with P11-P14 experiencing blast crisis. Point mutations in the BCR-ABL kinase domain were observed in P7 (F311I mutation), P8 (T315I mutation), and P13 (G250E mutation).

As depicted in **Figure 4**, while both the nanocore (anti-BCR-ABL PS-siRNA) and nanoshell (Tf-Soraf) showed improved cytotoxicity compared to free drug controls, approximately 40-60% of cells remained viable in nearly all patient samples. Notably, the effect of the Tf-Soraf nanoshell was more pronounced in the cells isolated from the resistant patients (P8-P14) compared to those in the chronic phase (P1-P7), likely due to the increased expression of STAT5 and TfR1 in the resistant cases.

In Vivo Anti-Tumor Activity of CS-NPs in a CML Xenograft Model

The *in vivo* anti-tumor efficacy of CS-NPs was evaluated using a mouse model of refractory CML after assessing acute toxicity in healthy Swiss albino mice (**Supplementary Figure S5**). Despite STAT5's crucial role in blood cell formation, CS-NPs displayed minimal cytotoxicity to CD34+ bone marrow progenitors and healthy blood cells at the tested concentrations

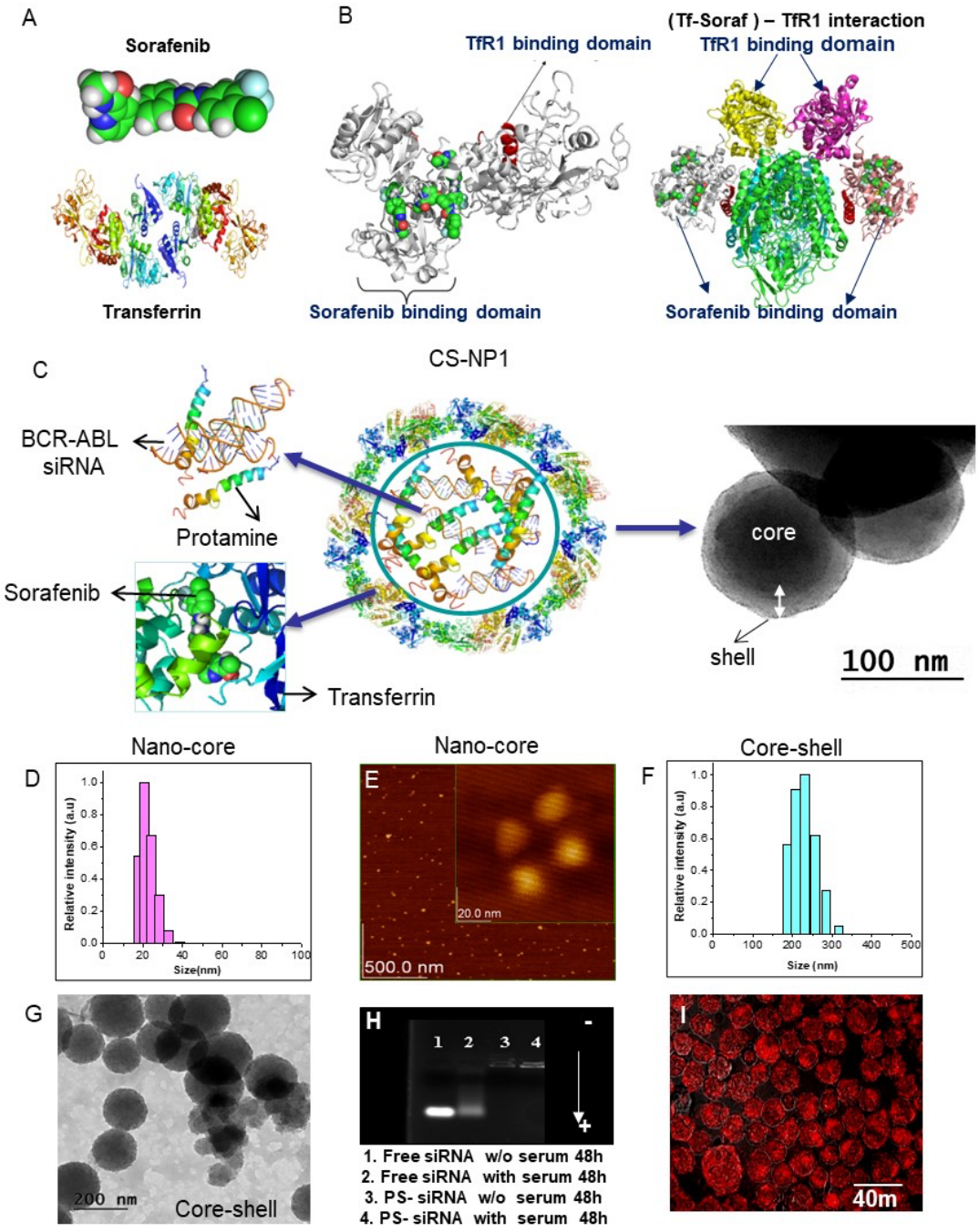

Figure 2. In-silico design, characterization, and optimization of (PS-siRNA) -(Tf-Soraf) core-shell nanoparticles (CS-NP1). (A) In-silico modeling of transferrin-sorafenib nanoshell conducted using AutoDock 4.2. (B) In-silico modeling of Tf-Soraf shows that the sorafenib binding domain in Tf and receptor binding site for TfR1 are different; sorafenib loading in Tf does not interfere with the interactions of Tf with TfR1. (C) Schematic representation of core-shell nanomedicine comprising of PS-siRNA nanocore and Tf-Soraf nanoshell. Transmission electron microscopic (TEM) imaging shows the distinct phase of the core and the shell (D) Dynamic light scattering (DLS) shows the size distribution of the PS-siRNA nanocore. (E) atomic force microscopic (AFM) imaging of PS-siRNA nanocore, inset shows representative magnified image indicating ~ 20 nm sized PS-siRNA nanocomplex. (F) DLS shows a shift in the size distribution after nanoshell formation in CS-NP1. (G) TEM image of CS-NP1 showing particles of average size ~ 225 nm, (H) Serum stability of PS-siRNA nanocore compared with that of free siRNA. (I) Cellular uptake of fluorescent Au-nanocluster doped CS-NP1 showing bright red fluorescence emerging from the nanoparticles in the cytosol.

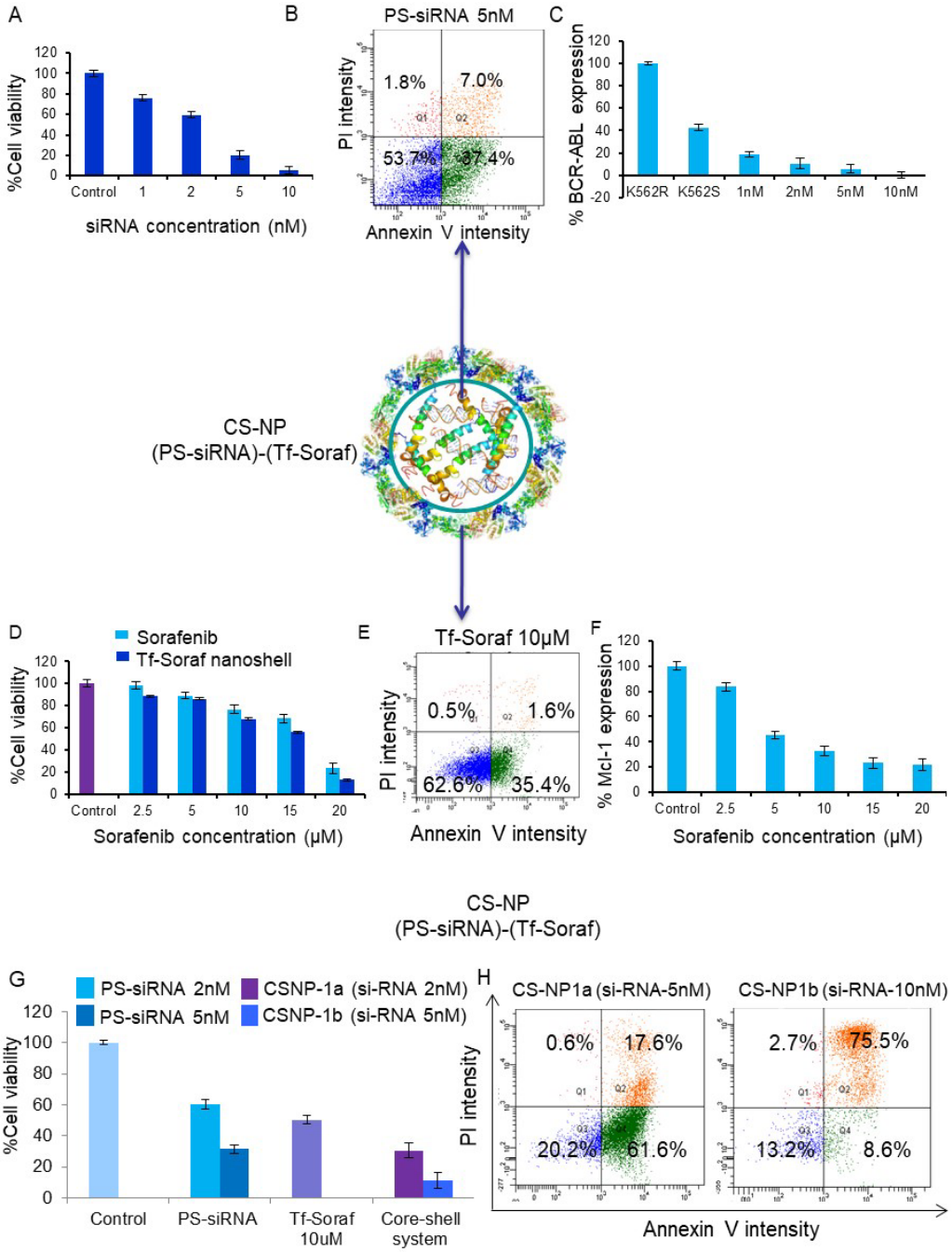

Figure 3. CS-NPs caused enhanced BCR-ABL silencing/inhibition and STAT5 inhibition. (A) MTT assay demonstrating the cell viability of K562R cells treated with PS-siRNA nanocore containing 1, 2, 5, or 10 nM siRNA for 48 hours under culture conditions. Untreated cells served as the control. (B) A representative flow cytometry plot shows apoptosis induced by PS-siRNA nanocore. (C) Graph depicting the percentage downregulation of BCR-ABL gene expression with and without PS-siRNA nanocore treatment over 48 hours. (D) MTT assay illustrating the cell viability of K562R cells treated with Tf-Soraf nanoshell containing 2.5-20 μM sorafenib, compared to free sorafenib, over 48 hours under culture conditions. (E) Representative flow cytometry plot showing apoptosis induced by Tf-Soraf nanoshell with 10 μM sorafenib. (F) The graph shows the percentage of downregulation of Mcl-1 gene expression, which is an immediate target of STAT5. (G) MTT assay displaying the reduced viability of K562R cells treated with CS-NPs over 48 hours, compared to treatment with either the nanocore or nanoshell alone. (H) Representative flow cytometry plot illustrating apoptosis induced by chitosan nanoparticles over 48 hours. Untreated cells were used as the control.

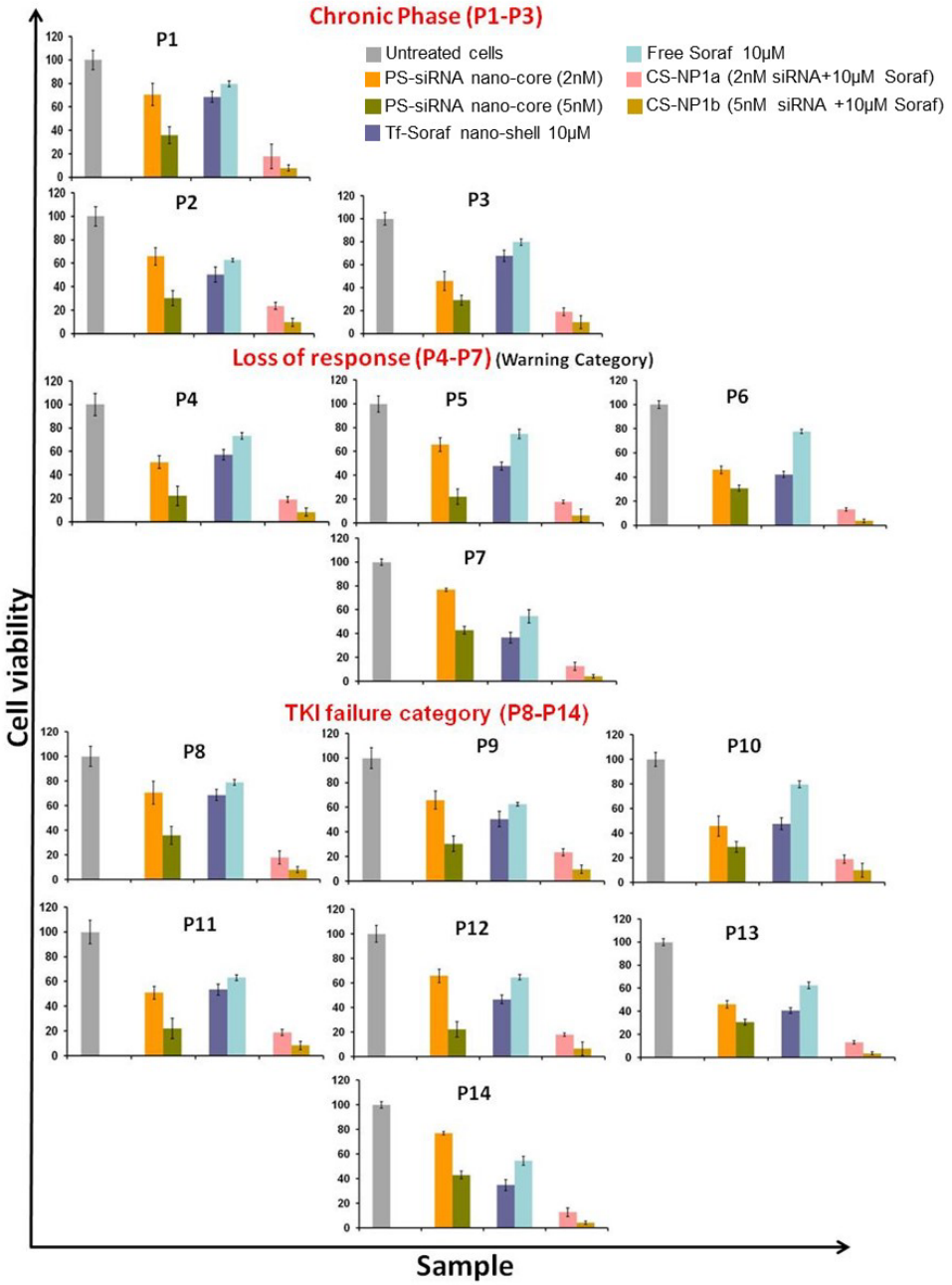

Figure 4. Chitosan nanoparticles (CS-NP) induced enhanced toxicity in leukemic cells isolated from chronic myeloid leukemia (CML) patients. MTT assay of leukemic cells isolated from peripheral blood/bone marrow of CML patients (n=14) treated with PS-siRNA (2 nM and 5 nM siRNA), Bare sorafenib, Tf-Soraf nanoshell (10 μM sorafenib), CS-NPs for 48 h under culture conditions. Chitosan CS-NPs treated were of two concentrations with PS-si-RNA nanocore, 2 nM& 5 nM, while retaining 10 μM sorafenib in a nanoshell. P1-P3 were chronic phase drug-sensitive patients, P4-P7 were patients who had started to show loss of response to imatinib, and P8-P14 were not responding to second-line dasatinib. Untreated cells were used as control.

Histopathological analysis of subcutaneously grown CML tumors in Swiss albino nu/nu mice revealed a uniform tumor mass, as shown in **Figure 5A**. FISH analysis confirmed the presence of BCR-ABL translocation in the tumor cells (**Figure 5B**). qRT-PCR demonstrated significant fold changes in BCR-ABL, STAT5A, and STAT5B expression, indicating overexpression of these driver mechanisms in the xenograft (**Figure 5C**).

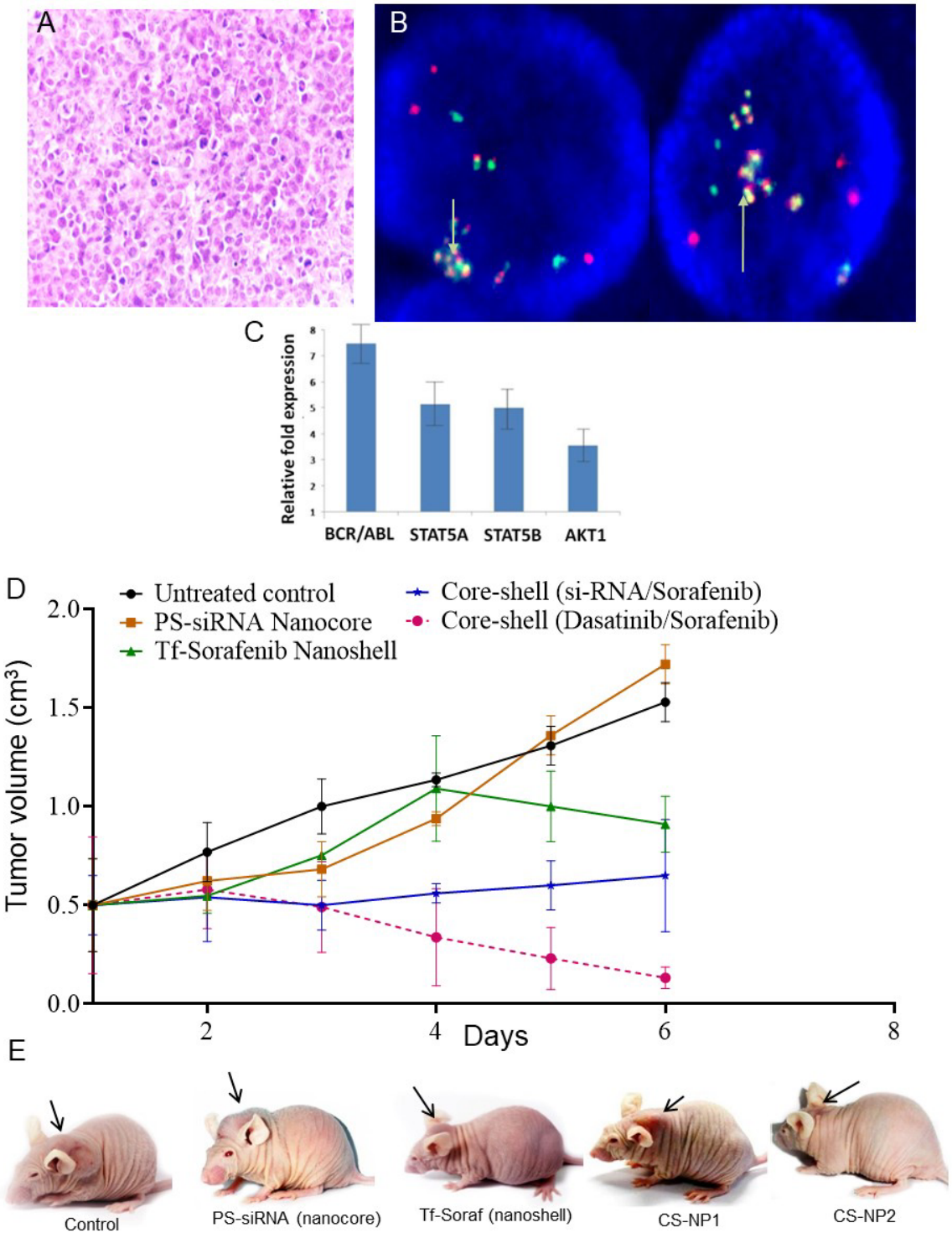

Figure 5. Anti-leukemic studies of chitosan nanoparticles (CS-NPs) in subcutaneous xenograft mice model. (A) H&E image showing the tissue homology (B) FISH analysis for the conformation of BCR-ABL fusion from single cell suspension of tumor mass. (C) mRNA level studies indicating fold changes in the expression of BCR-ABL, STAT5A & B. (D) Graph showing the reduction in tumor volume after intratumoral treatment with nanocore (PS-siRNA, 1 mg/kg), nanoshell (Tf-Soraf, 20 mg/kg sorafenib), CS-NP1 (PS-siRNA/Sorafenib) and CS-NP2 (da-satinib/sorafenib). Statistical analysis using one-way ANOVA was done. (E) Representative animal images on the 20th day after 5-day intratumoral treatment are shown above.

To test the anti-tumor efficacy, CS-NPs were administered to separate groups of mice (n = 3) for 5 days, with a dosage equivalent to 1 mg/kg siRNA in the nanocore and 20 mg/kg sorafenib in the nanoshell for CS-NP1. To align with current clinical practices, we also prepared another core-shell nanoparticle, replacing siRNA with the clinically used drug dasatinib in the core while retaining the Tf-Soraf nanoshell (**Supplementary Figure 6)**. The *in-silico* model of the Albumin-dasatinib-Tf-sorafenib core-shell nanoparticle (CS-NP2), formed by the sequential precipitation of albumin-dasatinib nanocore followed by the controlled precipitation of transferrin-sorafenib nanoshell, revealed spherical nanocore particles with an average size of approximately 60 nm (**Supplementary Figure S7A & B**). DLS analysis confirmed the sequential formation of core and core-shell particles, with sizes of ~ 45±17 nm for the core and 158±30 nm for the core-shell (**Supplementary Figure S7D, E & F**). TfR1-targeted uptake of CS-NP2 in the Tf overexpressing CML cell line K562R is illustrated in **Supplementary Figure S7G & Supplementary Figure S4 (last panel)**. CS-NP2 was tested in the xenograft model with dosages of 10 mg/kg dasatinib and 10 mg/kg sorafenib.

Figure 5D shows the tumor regression patterns in the CS-NP1 (PS-siRNA-Tf-Sorafenib) treated group compared to controls. Tumor regression was notably more significant with the Tf-Soraf nanoshell than with the PS-siRNA nanocore. Nonetheless, CS-NP1 demonstrated superior tumor reduction compared to controls, indicating that the combinatorial therapy of BCR-ABL gene silencing and STAT5 inhibition is more effective than either free drugs or individual nano-drugs alone. The enhanced efficacy of CS-NP1 was obvious compared to both the PS-siRNA nanocore and the Tf-Sorafenib nanoshell. Finally, the efficacy of CS-NP2, which includes a dasatinib-sorafenib combination, is shown in **Figure 5E** through representative images of animals treated with controls, CS-NP1, and CS-NP2.

Notably, tumor reduction effects were significantly more pronounced with CS-NP2 than the siRNA-based CS-NP1. CS-NP2 consisted of dasatinib, a highly potent inhibitor for BCR-ABL with IC50 ~ 5 nm than imatinib (IC50 = 600 nm), and STAT5 inhibitor sorafenib in the shell, giving a combinatorial anti-tumor effect. Further, dasatinib has better chemical stability in the physiological medium than the relatively unstable siRNA molecules. CS-NP2 demonstrated statistically significant tumor reduction ($p < 0.008$) compared to untreated controls.

The *in vivo* anti-tumor effects of CS-NPs in xenograft models of refractory CML, characterized by BCR-ABL-STAT5-TfR1 overexpression, were consistent with the *in vitro* data from patient samples. CS-NP1 and CS-NP2 exhibited excellent anti-tumor activity; however, CS-NP2, including the clinically relevant dasatinib-sorafenib combination, showed superior efficacy. This underscores the potential of using novel nanomedicine architectures loaded with clinically approved drugs to target multiple oncogenic pathways simultaneously.

Conclusion

It has been nearly two decades since the discovery of imatinib mesylate for treating BCR-ABL$^+$ CML. Although CML is managed with later-generation kinase inhibitors, many patients still resist or relapse when leukemic cells rely on alternative proteins for survival. While nanoparticles have been extensively utilized for various clinical applications, overcoming the limitations of free therapeutics and successfully navigating cellular, systemic, and micro-environmental barriers, a critical need remains to advance their use in personalized, multi-targeted nanotherapeutics.

Instead of a “one-size-fits-all” approach, the design and development of nanotherapeutics should be guided by molecular diagnosis and patient heterogeneity. With this approach in mind, we designed a protein-protein core-shell nanomedicine capable of targeting two mechanistic pathways simultaneously in refractory CML. Refractory CML is associated with several complementary mechanisms, possibly BCR-ABL dependent or independent. Dose escalation of standard drugs such as imatinib or newer BCR-ABL kinase inhibitors such as dasatinib, nilotinib, and ponatinib can partially address BCR-ABL dependent mechanisms.[24] However, independent activation of survival pathways like STAT5 and their interactions with anti-apoptotic proteins exacerbate the situation and remain largely unaddressed. Our

goal was to simultaneously target both BCR-ABL and STAT5 together using rationally designed core-shell nanoparticles.

We used unique protein-protein core-shell nanoparticles based on protamine-transferrin or albumin-transferrin combinations to simultaneously deliver the SMI payload intracellularly and in a targeted fashion. Importantly, the choice of transferrin for cellular targeting via TfR1 was based on the molecular phenotype of imatinib-resistant patients. Our results on the refractory cell line, patient-derived primary CML cells, and xenograft models demonstrated the advantage of combinatorial targeting of BCR-ABL and STAT5 to overcome drug resistance. Our results indicate that the rational design of core-shell nanomedicines can successfully target multiple oncogenic pathways in cancer.

Acknowledgments: The authors thank Amrita University for providing the infrastructure and research facilities and the Hematology Department, Amrita Institute of Medical Sciences and Research Centre, for providing patient samples.

Funding: The authors thank the Department of Biotechnology, Government of India, for financial support under the project Translational Protein Nanomedicine (BT/PR7665/NNT/28/658/2013).

Author Contributions: APR and LGK had equal contributions in all experiments and writing the paper, NS had done clinical and molecular diagnosis of the patients and helped in planning the research, GLM performed the computational modeling and docking studies, PLH conducted gene expression studies, MVGT conducted cytogenetic characterization of the patients, DM helped in planning and designing of experiments, KM helped in conducting protein expression studies, PK helped in clinical and molecular diagnosis of the patients and helped planning the research, SN and MK supervised the study and executed the experimental design.

Conflicts of Interest: The authors declare no conflict of interest. The funders had no role in the study's design, data collection, analysis, interpretation, manuscript writing, or decision to publish the results. For a written statement, please contact the journal office editor@precisionnanomedicine.com.

Quote this article as Retnakumary AP, Kumar LG, Sidharthan N, Keechilat P, Malarvizhi GL, Hanumanthu PL, Thampi MV, Menon D, Menon K, Nair S, and Koyakutty M, Self-assembled Human Serum Protein-based Core-shell Nanoparticles to Inhibit Key Oncogenic Signaling in Drug-Resistant Leukemia, Precis. Nanomed. 2024, 7(4):1348-1364, https://doi.org/10.33218/001c.125335.

References

1. Liu GH, Chen T, Zhang X, Ma XL, Shi HS. Small molecule inhibitors targeting the cancers. MedComm. 2022 Dec;3(4):e181.
2. Pottier C, Fresnais M, Gilon M, Jérusalem G, Longuespée R, Sounni NE. Tyrosine Kinase Inhibitors in Cancer: Breakthrough and Challenges of Targeted Therapy. Cancers. 2020 Mar 20;12(3):731.
3. Wu PS, Lin MH, Hsiao JC, Lin PY, Pan SH, Chen YJ. EGFR-T790M Mutation-Derived Interactome Rerouted EGFR Translocation Contributing to Gefitinib Resistance in Non-Small Cell Lung Cancer. Mol Cell Proteomics MCP. 2023 Sep;22(9):100624.
4. Apperley JF. Part I: Mechanisms of resistance to imatinib in chronic myeloid leukemia. Lancet Oncol. 2007 Nov 1;8(11):1018–29.
5. Noguchi K, Ikawa Y, Takenaka M, Sakai Y, Fujiki T, Kuroda R, et al. Acquired L1196M ALK mutation in anaplastic lymphoma kinase-positive anaplastic large cell lymphoma during alectinib administration. EJHaem. 2023 Feb;4(1):305–8.
6. Hu, C., Mi, W., Li, F. et al. Optimizing drug combination and mechanism analysis based on risk pathway crosstalk in pan-cancer. Sci Data 11, 74 (2024). https://doi.org/10.1038/s41597-024-02915-y

7. Garg P, Malhotra J, Kulkarni P, Horne D, Salgia R, Singhal SS. Emerging Therapeutic Strategies to Overcome Drug Resistance in Cancer Cells.
8. Retnakumari AP, Hanumanthu PL, Malarvizhi GL, Prabhu R, Sidharthan N, Thampi MV, et al. Rationally Designed Aberrant Kinase-Targeted Endogenous Protein Nanomedicine against Oncogene Mutated/Amplified Refractory Chronic Myeloid Leukemia. Mol Pharm. 2012 Nov 5;9(11):3062–78.
9. Chandran P, Gupta N, Retnakumari AP, Malarvizhi GL, Keechilat P, Nair S, et al. Simultaneous inhibition of aberrant cancer kinome using rationally designed polymer-protein core-shell nanomedicine. Nanomedicine NanotechnolBiol Med. 2013 Nov 1;9(8):1317–27.
10. Zhang H, Wu JH, Xue HZ, Zhang R, Yang ZS, Gao S, et al. Biomimetically constructing a hypoxia-activated programmable phototheranostics at the molecular level. Chem Sci. 13(31):8979–88.
11. Deshpande S, Sharma S, Koul V, Singh N. Core–Shell Nanoparticles as an Efficient, Sustained, and Triggered Drug-Delivery System. ACS Omega 2017 2 (10), 6455-6463 Available from: https://pubs.acs.org/doi/10.1021/acsomega.7b01016
12. Kovács, D., Igaz, N., Marton, A. et al. Core–shell nanoparticles suppress metastasis and modify the tumour-supportive activity of cancer-associated fibroblasts. J Nanobiotechnol 18, 18 (2020). https://doi.org/10.1186/s12951-020-0576-x
13. Menon JU, Kuriakose A, Iyer R, Hernandez E, Gandee L, Zhang S, et al. Dual-Drug Containing Core-Shell Nanoparticles for Lung Cancer Therapy. Sci Rep. 2017 Oct 16;7(1):13249.
14. Malarvizhi GL, Retnakumari AP, Nair S, Koyakutty M. Transferrin targeted core-shell nanomedicine for combinatorial delivery of doxorubicin and sorafenib against hepatocellular carcinoma. Nanomedicine NanotechnolBiol Med. 2014 Nov;10(8):1649–59.
15. Narayanan S, Mony U, Vijaykumar DK, Koyakutty M, Paul-Prasanth B, Menon D. Sequential release of epigallocatechin gallate and paclitaxel from PLGA-casein core/shell nanoparticles sensitizes drug-resistant breast cancer cells. Nanomedicine NanotechnolBiol Med. 2015 Aug;11(6):1399–406.
16. Narayanan S, Pavithran M, Viswanath A, Narayanan D, Mohan CC, Manzoor K, et al. Sequentially releasing dual-drug-loaded PLGA–casein core/shell nanomedicine: Design, synthesis, biocompatibility and pharmacokinetics. Acta Biomater. 2014 May 1;10(5):2112–24.
17. Cardama A Q, Cortes J; Molecular biology of bcr-abl1–positive chronic myeloid leukemia. Blood 2009; 113 (8): 1619–1630. doi: https://doi.org/10.1182/blood-2008-03-144790
18. Faderl S, Talpaz M, Estrov Z, O'Brien S, Kurzrock R, Kantarjian H M. The Biology of Chronic Myeloid Leukemia. N Engl J Med 1999;341:164-172.DOI: 10.1056/NEJM199907153410306.
19. O'Hare T, Eide CA, Deininger MWN. Bcr-Abl kinase domain mutations, drug resistance, and the road to a cure for chronic myeloid leukemia. Blood. 2007 Oct 1;110(7):2242–9.
20. Weisberg E, Griffin JD. Mechanism of resistance to the ABL tyrosine kinase inhibitor STI571 in BCR/ABL-transformed hematopoietic cell lines. Blood. 2000 Jun 1;95(11):3498–505.
21. Mahon FX, Deininger MWN, Schultheis B, Chabrol J, Reiffers J, Goldman JM, et al. Selection and characterization of BCR-ABL positive cell lines with differential sensitivity to the tyrosine kinase inhibitor STI571: diverse mechanisms of resistance. Blood. 2000 Aug 1;96(3):1070–9.
22. Saglio G, Hochhaus A, Goh YT, Masszi T, Pasquini R, Maloisel F, et al. Dasatinib in Imatinib-Resistant or Imatinib-Intolerant Chronic Myeloid Leukemia in Blast Phase After 2 Years of Follow-Up in a Phase 3 Study. Cancer. 2010 Aug 15;116(16):3852–61.
23. Ottmann, O., Larson, R., Kantarjian, H. et al. Phase II study of nilotinib in patients with relapsed or refractory Philadelphia chromosome—positive acute lymphoblastic leukemia. Leukemia 27, 1411–1413 (2013). https://doi.org/10.1038/leu.2012.324
24. Hughes TP, Saglio G, Quintás-Cardama A, Mauro MJ, Kim DW, Lipton JH, et al. BCR-ABL1 mutation development during first-line treatment with dasatinib or imatinib for chronic myeloid leukemia in chronic phase. Leukemia. 2015 Sep;29(9):1832–8.
25. Mahon FX, Hayette S, Lagarde V, Belloc F, Turcq B, Nicolini F, et al. Evidence that resistance to nilotinib may be due to BCR-ABL, Pgp, or Src kinase overexpression. Cancer Res. 2008 Dec 1; 68(23):9809-16. doi: 10.1158/0008-5472.CAN-08-1008.

26. Iqbal N, Iqbal N. Imatinib: A Breakthrough of Targeted Therapy in Cancer. Chemother Res Pract. 2014; 2014:357027.
27. O'Hare T, Shakespeare WC, Zhu X, Eide CA, Rivera VM, Wang F, et al. AP24534, a Pan-BCR-ABL Inhibitor for Chronic Myeloid Leukemia, Potently Inhibits the T315I Mutant and Overcomes Mutation-Based Resistance. Cancer Cell. 2009 Nov 3;16(5):401–12.
28. Cortes JE, Kantarjian HM, Brümmendorf TH, Kim DW, Turkina AG, Shen ZX, et al. Safety and efficacy of bosutinib (SKI-606) in chronic phase Philadelphia chromosome-positive chronic myeloid leukemia patients with resistance or intolerance to imatinib. Blood. 2011 Oct 27;118(17):4567–76.
29. Hochhaus A, Kantarjian H. The development of dasatinib as a treatment for chronic myeloid leukemia (CML): from initial studies to application in newly diagnosed patients. J Cancer Res Clin Oncol. 2013 Dec; 139(12):1971–84.
30. Okabe S, Tauchi T, Ohyashiki K. Characteristics of dasatinib- and imatinib-resistant chronic myelogenous leukemia cells. Clin Cancer Res. 2008 Oct 1;14(19):6181-6. doi: 10.1158/1078-0432.CCR-08-0461.
31. Grebien F, Hantschel O, Wojcik J, Kaupe I, Kovacic B, Wyrzucki AM, et al. Targeting the SH2-Kinase Interface in Bcr-Abl Inhibits Leukemogenesis. Cell. 2011 Oct 14;147(2):306–19.
32. Warsch W, Walz C, Sexl V. JAK of all trades: JAK2-STAT5 as novel therapeutic targets in BCR-ABL1+ chronic myeloid leukemia. Blood. 2013 Sep 26;122(13):2167–75.
33. Halim CE, Deng S, Ong MS, Yap CT. Involvement of STAT5 in Oncogenesis. Biomedicines. 2020 Sep;8(9):316.
34. Coffer PJ, Koenderman L, de Groot RP. The role of STATs in myeloid differentiation and leukemia. Oncogene. 2000 May 15;19(21):2511-22. doi: 10.1038/sj.onc.1203479. PMID: 10851050.
35. Hoelbl A, Schuster C, Kovacic B, Zhu B, Wickre M, Hoelzl MA, et al. Stat5 is indispensable for the maintenance of bcr/abl-positive leukaemia. EMBO Mol Med. 2010 Mar;2(3):98–110.
36. Ma L, Shan Y, Bai R, Xue L, Eide CA, Ou J et al. A therapeutically targetable mechanism of BCR-ABL-independent imatinib resistance in chronic myeloid leukemia. Sci Transl Med. 2014 Sep 3;6(252):252ra121. doi: 10.1126/scitranslmed.3009073.
37. Hantschel, O., Warsch, W., Eckelhart, E. et al. BCR-ABL uncouples canonical JAK2-STAT5 signaling in chronic myeloid leukemia. Nat Chem Biol 8, 285–293 (2012). https://doi.org/10.1038/nchembio.775
38. Warsch W, Kollmann K, Eckelhart E, Fajmann S, Cerny-Reiterer S, Hölbl A, et al. High STAT5 levels mediate imatinib resistance and indicate disease progression in chronic myeloid leukemia. Blood. 2011 Mar 24;117(12):3409–20.
39. Warsch W, Grundschober E, Berger A, Gille L, Cerny-Reiterer S, Tigan AS, et al. STAT5 triggers BCR-ABL1 mutation by mediating ROS production in chronic myeloid leukaemia. Oncotarget. 2012 Dec;3(12):1669-87. doi: 10.18632/oncotarget.806.
40. Zhang X, Tu H, Yang Y, Jiang X, Hu X, Luo Q, et al. Bone marrow-derived mesenchymal stromal cells promote resistance to tyrosine kinase inhibitors in chronic myeloid leukemia via the IL-7/JAK1/STAT5 pathway. J Biol Chem. 2019 Aug 9;294(32):12167-12179. doi: 10.1074/jbc.RA119.008037.
41. Wang X, Yang J, Guo G, Feng R, Chen K, Liao Y, et al. Novel lncRNA-IUR suppresses Bcr-Abl-induced tumorigenesis through regulation of STAT5-CD71 pathway. Mol Cancer. 2019 Apr 8;18(1):84. doi: 10.1186/s12943-019-1013-3.
42. Nie ZY, Yao M, Yang Z, Yang L, Liu XJ, Yu J, et al. De-regulated STAT5A/miR-202-5p/USP15/Caspase-6 regulatory axis suppresses CML cell apoptosis and contributes to Imatinib resistance. J Exp Clin Cancer Res. 2020 Jan 17;39(1):17. doi: 10.1186/s13046-019-1502-7.
43. Yin L, Xu J, Wu W, Niu M, Li Z, Zhu F, et al. Dual inhibition of STAT3 and STAT5 may overcome imatinib resistance in chronic myeloid leukemia. Hematology. 2023 Dec;28(1):2224625. doi: 10.1080/16078454.2023.2224625.
44. Xu X, Zhang X, Liu Y, Yang L, Huang S, Lu L, et al. BM microenvironmental protection of CML cells from imatinib through Stat5/NF-κBsignaling and reversal by Wogonin. Oncotarget. 2016 Mar 24;7(17):24436–54.

45. Zhang C. Essential functions of iron-requiring proteins in DNA replication, repair and cell cycle control. Protein Cell. 2014 Oct;5(10):750-60. doi: 10.1007/s13238-014-0083-7.
46. Forciniti S, Greco L, Grizzi F, Malesci A, Laghi L. Iron Metabolism in Cancer Progression. Int J Mol Sci. 2020 Mar 24;21(6):2257. doi: 10.3390/ijms21062257.
47. Kazan HH, Urfali-Mamatoglu C, Gunduz U. Iron metabolism and drug resistance in cancer. Bio-Metals. 2017 Oct 1;30(5):629–41.
48. Shen L, Zhou Y, He H, Chen W, Lenahan C, Li X, et al. Crosstalk between Macrophages, T Cells, and Iron Metabolism in Tumor Microenvironment. Oxid Med Cell Longev. 2021 Feb 2;2021:8865791. doi: 10.1155/2021/8865791.
49. DeRosa A, Leftin A. The Iron Curtain: Macrophages at the Interface of Systemic and Microenvironmental Iron Metabolism and Immune Response in Cancer. Front Immunol. 2021 Apr 27;12:614294. doi: 10.3389/fimmu.2021.614294.
50. Zhu BM, McLaughlin SK, Na R, Liu J, Cui Y, Martin C, et al. Hematopoietic-specific Stat5-null mice display microcytic hypochromic anemia associated with reduced transferrin receptor gene expression. Blood. 2008 Sep 1;112(5):2071-80. doi: 10.1182/blood-2007-12-127480.
51. Kerenyi MA, Grebien F, Gehart H, Schifrer M, Artaker M, Kovacic B, et al. Stat5 regulates cellular iron uptake of erythroid cells via IRP-2 and TfR-1. Blood. 2008 Nov 1;112(9):3878–88.
52. Wang HW, Ma KL, Liu H, Zhou JY. Reversal of multidrug resistance in leukemia cells using a transferrin-modified nanomicelle encapsulating both doxorubicin and psoralen. Aging. 2020 Apr 7;12(7):6018–29.
53. Lilin Zhang, Fumiko Nomura, Yoichi Aikawa, Yoshikazu Kurosawa, Kazuhiro Morishita, Yukio Sudo; Abstract 5586: PPMX-T003, a fully human anti-TfR1 antibody with potent efficacy against hematologic malignancies. Cancer Res 1 July 2017; 77 (13_Supplement): 5586. https://doi.org/10.1158/1538-7445.AM2017-5586
54. Schafranek L, Nievergall E, Powell JA, Hiwase DK, Leclercq T, Hughes TP, et al. Sustained inhibition of STAT5, but not JAK2, is essential for TKI-induced cell death in chronic myeloid leukemia. Leukemia. 2015 Jan;29(1):76–85.
55. Retnakumari A, Setua S, Menon D, Ravindran P, Muhammed H, Pradeep T, et al. Molecular-receptor-specific, non-toxic, near-infrared-emitting Au cluster-protein nanoconjugates for targeted cancer imaging. Nanotechnology. 2009 Dec;21(5):055103.
56. Senapati J, Sasaki K, Issa GC, Lipton JH, Radich JP, Jabbour E, et al. Management of chronic myeloid leukemia in 2023 - common ground and common sense. Blood Cancer J. 2023 Apr 24;13(1):58. doi: 10.1038/s41408-023-00823-9.